Demonstration of a Circularly Polarized Plasma-Based Soft-X-Ray Laser

A. Depresseux, E. Oliva, J. Gautier, F. Tissandier, G. Lambert, B. Vodungbo, J-P. Goddet, A. Tafzi, J. Nejdl, M. Kozlova, et al.

Demonstration of a Circularly Polarized Plasma-Based Soft-X-Ray Laser

A. Depresseux,[1] E. Oliva,[2] J. Gautier,[1] F. Tissandier,[1] G. Lambert,[1] B. Vodungbo,[1] J-P. Goddet,[1] A. Tafzi,[1] J. Nejdl,[3] M. Kozlova,[3] G. Maynard,[2] H. T. Kim,[4,5] K. Ta Phuoc,[1] A. Rousse,[1] P. Zeitoun,[1] and S. Sebban[1]

[1]*Laboratoire d'Optique Appliquée, ENSTA ParisTech, CNRS, École Polytechnique, Université Paris-Saclay, 828 boulevard des Maréchaux, 91762 Palaiseau, France*

[2]*Laboratoire de Physique des Gaz et des Plasmas, CNRS Université Paris-Sud 11, 91405, Orsay, France*

[3]*ELI Beamlines Project, Institute of Physics of the ASCR, Na Slovance 2, 182 21 Prague 8, Czech Republic*

[4]*Advanced Photonics Research Institute, GIST, Gwangju 500-712, Korea*

[5]*Center for Relativistic Laser Science, Institute for Basic Science (IBS), Gwangju 500-712, Korea*

(Received 27 May 2015; published 19 August 2015)

We report the first experimental demonstration of a laser-driven circularly polarized soft-x-ray laser chain. It has been achieved by seeding a 32.8 nm Kr IX plasma amplifier with a high-order harmonic beam, which has been circularly polarized using a four-reflector polarizer. Our measurements testify that the amplified radiation maintains the initial polarization of the seed pulse in good agreement with our Maxwell-Bloch modeling. The resulting fully circular soft-x-ray laser beam exhibits a Gaussian profile and yields about 10^{10} photons per shot, fulfilling the requirements for laboratory-scale photon-demanding application experiments.

DOI: 10.1103/PhysRevLett.115.083901 PACS numbers: 42.55.Vc, 42.50.Md, 42.65.Ky

Controlling the state of polarization of soft-x-ray sources is a powerful approach for probing material structures, along with their electronic and magnetic properties. In this framework, areas of study involve dichroism [1], magnetization dynamics in matter [2], or chiral domains in biology and molecular physics [3,4]. In the soft-x-ray range, the availability of coherent circularly polarized light has been limited so far to a few large-scale facilities and more recently to high-order harmonic (HH) generation. Regarding HH, several techniques have successfully been demonstrated, including the use of prealigned molecules as targets [5], a circularly polarized counterrotating bichromatic driver [6], a cross-polarized two-color laser field [7], or resonant high-order harmonic generation [8]. However, the photon yield remains low, which turns those sources inopportune for single-shot measurements. Higher photon flux has been demonstrated on large-scale facilities, such as synchrotrons [9] and free-electron lasers [10–12], by modifying the configuration of the undulators. Notwithstanding, such techniques turn out to be expensive and complex, thus preventing a flexible and wide-access utilization. To fill the gap between HH sources and large-scale facilities, collisional soft-x-ray lasers (SXRLs) offer a promising approach for generating compact but photon-rich circularly polarized light allowing photon-demanding measurements at the laboratory scale [13]. Despite one proposal based on Zeeman splitting of the $3d^9 4d_{J=0} \mapsto 3d^9 4p_{J=1}$ transition of the nickel-like molybdenum ions at 18.895 nm [14], the polarization of existing SXRL sources has been either undefined or restricted to be linear so far [15,16].

For generating circularly polarized SXRL beams, we propose here a new approach based on the seeding of a laser-driven optical field ionization soft-x-ray plasma amplifier by a circularly polarized HH at 32.8 nm. Figure 1 shows the Kastler diagram of the SXRL using the Ni-like krypton ions. The XRL is generated between the $3d^9 4d_{J=0} \mapsto 3d^9 4p_{J=1}$ levels. The lower level of the electric dipole laser transition has three degenerate sublevels ($m = -1, 0, 1$). Because of the selection rules from quantum theory, each sublevel can interact only with a particular component of the electric field, which can be decomposed into eigencomponents, namely, left- or right-handed circular polarizations. The resonant transitions between the upper level (u) and lower levels ($l, -1$) and ($l, 1$) involves only the left-handed and right-handed circular polarization components of the electric field, respectively. The purple double arrows stand for the resonant transitions that can be preferentially excited with left-handed circular (LHC) or right-handed circular

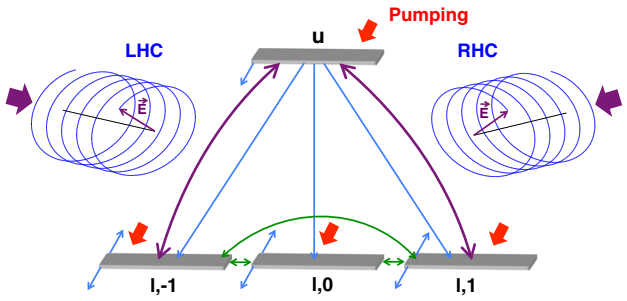

FIG. 1 (color online). Atomic structure of the laser Kr^{8+} transition with its lower sublevels ($m = +1, 0, -1$) and the associated physical processes.

polarization between the upper level (u) and the $(l,-1)$ or $(l,1)$ lower level, respectively. The blue arrows illustrate the various depopulation processes, whereas the green double arrows describe the population transfers between sublevels. In an amplified spontaneous emission (ASE) mode, emission is unpolarized. However, the polarization of amplified injection-seeded HH corresponds to the polarization of the seed, whose components preferentially excite a particular transition. As a consequence, one could expect to efficiently generate a coherent circularly polarized soft-x-ray laser beam (CPSXRL) [17] when seeding the $3d^9 4d_{J=0} \mapsto 3d^9 4p_{J=1}$ SXRL transition by circularly polarized light.

In this Letter, we report the first experimental demonstration of a circularly polarized plasma-based soft-x-ray laser by implementing a grazing incidence phase shifter into a soft-x-ray laser chain composed by a HH seed and a 32.8 nm population-inverted plasma amplifier (Fig. 2). The experiment has been carried out at the Laboratoire d'Optique Appliquée. To generate the soft-x-ray amplifier, a circularly polarized 1.36 J, 30 fs pump beam is focused into a gas cell filled with 30 mbar of krypton using a 75 cm focal length spherical mirror. The laser intensity at the focus is of the order of 2×10^{18} W/cm^2. A 5-mm-long optical field ionized amplifying plasma column is therefore generated and pumped through collisional excitation [18]. A second laser beam (16 mJ, 350 fs) is used to generate the high-order harmonics seed in another gas cell filled with 30 mbar argon. The 25th harmonic signal has been spectrally tuned to match the $3d^9 4d_{J=0} \mapsto 3d^9 4p_{J=1}$ transition at 32.8 nm by chirping [19] the laser driver. The seed beam is image relayed onto the entrance of the Kr^{8+} plasma using a grazing incidence toroidal mirror and synchronized with the pump beam to match the gain lifetime. In standard operation conditions, the amplified emission is composed by a highly collimated Gaussian-like beam with a divergence of about 1 mrad. Previous measurements have shown that the wave front is better than $\lambda/10$ [20] and that the duration of the amplified pulse is a few picoseconds [21].

To convert the HH polarization from linear to circular, a grazing incidence four-reflector phase shifter (polarizer) [22] and a $\lambda/2$ wave plate have been implemented between the HH seed and the amplifier. The phase shifter consists in four uncoated gold mirrors operating at 12° grazing incidence [23], which convert polarization from linear to circular. This method allows getting fully circularly polarized soft-x-ray radiation with an efficiency of about 1.5% at 32.8 nm [23]. The reflector angles of incidence are chosen to yield an overall phase shift of $\pi/2$ between p-and s-polarization components, whereas the polarization direction of the HH driving laser is adopted at 26.3° with respect to the p-polarization direction to equal both component field amplitudes. Its polarization direction is controlled thanks to a $\lambda/2$ wave plate on the infrared driver. The geometry takes into account the contributions from the image-relay system composed of a Pt-coated toroidal mirror and a SiO_2-coated plane mirror.

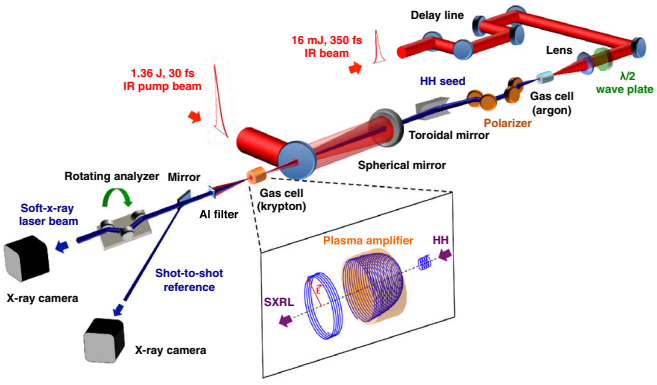

FIG. 2 (color online). Schematic description of the experimental setup.

The polarization of both the harmonics and the seeded soft-x-ray signal has been studied with the help of an analyzer consisting of three Mo(35 nm)/B4C(5 nm) multilayer mirrors in a 20°-40°-20° grazing incidence configuration. This motorized device could be rotated under vacuum from 0° to 90°. In the case of circularly polarized radiation generation, the analyzer transmission was found to be 1%, resulting in signal accumulation over 60 shots for polarization measurements. To measure the soft-x-ray yield of HH and seeded SXRL sources, we monitored the far-field emission using an on-axis 16-bit soft-x-ray CCD camera disposed 4.5 m away from the Kr IX plasma amplifier. The collection angle was about 5 mrad. We placed a 320 nm thin aluminum filter in the soft-x-ray beam path in order to block the infrared driving laser. Moreover, a plane mirror collected a part of soft x rays for a reference measurement to take into account the shot-to-shot signal fluctuations.

Figure 3 reports the measured output for both HH and seeded SXRL signals as a function of the analyzer rotation angle γ, in the cases of linear and circular polarization. The black crosses indicate the experimental measurements with their error bars, whereas the numerical fits are displayed by a blue and a red curve for linear and circular polarization, respectively. For linear polarization, the Malus law [23] has been recovered with the same contrast of about 7 between s and p transmissions for both the HH [Fig. 3(a)] and SXRL [Fig. 3(b)] signals, despite weak fluctuations that might originate from shot-to-shot pointing variations of the HH and SXRL. In the case of seeding with circularly polarized harmonics, the experimental results are shown in Figs. 3(c) and 3(d). Similarly to HH, the SXRL signal appears insensitive to the rotation of the analyzer, thus bearing testimony to either circularly polarized or unpolarized light.

We modeled the plasma amplification using a modified time-dependent Maxwell-Bloch code [24,25] taking into account the polarization of the seeding HH and including the transition lower sublevels. Our model

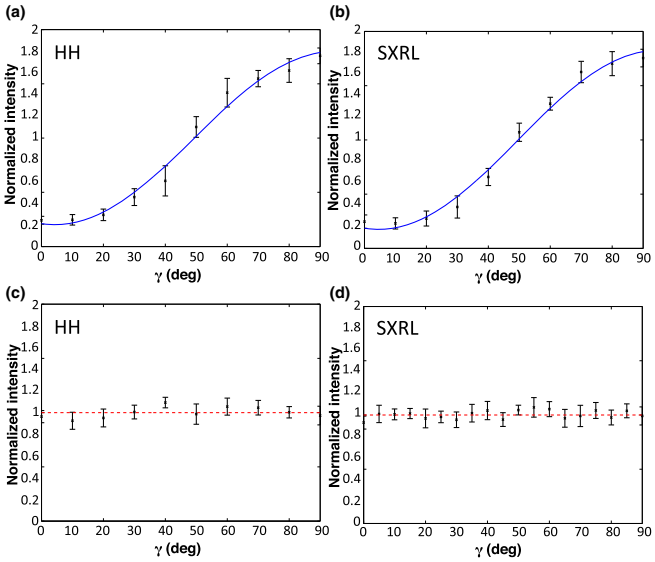

FIG. 3 (color online). Polarization investigation of the HH-seeded SXRL [(b),(d)] in the case of linearly (p) and circularly polarized high-order harmonics [(a),(c)], respectively.

describes the dynamics of the plasma population inversion between the laser transition upper level and its lower polarization-selected levels (see Fig. 1). This code solves the 1D paraxial Maxwell equation for the electric field in the slowly varying envelope approximation. This equation is supplemented with a constitutive relation for the polarization density, derived from Bloch equations $\mathbf{P} = \rho\mathbf{d}$, where ρ is the density operator and d the atomic electric dipole. Spontaneous emission is described as a stochastic source term Γ [26], and the populations of the lasing levels are modeled with standard rate equations. We use the collisional-radiative code OFIKinRad [27] to compute the radiative and collisional (de)excitation rates as long as the population of other atomic levels that strongly pump the lasing levels. To study the polarization of the amplified beam, the electric field is decomposed as a superposition of the right-handed and left-handed circularly polarized fields (E_L and E_R, respectively):

$$\frac{\partial E_{L,R}}{\partial \xi} = \frac{i\omega_0}{2c}\left[\mu_0 c^2 P_{L,R} - \frac{\omega_p^2}{\omega_0^2} E_{L,R}\right], \tag{1}$$

where ω_0 and ω_p are the HH and plasma frequencies, respectively, $P_{L,R}$ the polarization density, and $\xi = c\tau$, with $\tau = t - z/c$ the so-called reduced time. Selection rules imply that each field can interact only with a particular coherence [28]. Thus, the thrice-degenerate lower level of the lasing transition cannot be modeled as a whole but is split in three sublevels ($m = +1, 0, -1$) [29,30]. Elastic electron-ion collisions between sublevels are also considered via a population transfer rate γ_{PT} [30]:

$$\frac{\partial N_u}{\partial \tau} = \sum_k C_{k,u} N_k + \frac{1}{2\hbar}\mathrm{Im}(P_R E_R^* + P_L E_L^*), \tag{2}$$

$$\frac{\partial N_{l,1}}{\partial \tau} = \sum_k C_{k,1} N_k + \gamma_{\mathrm{PT}}(N_{l,-1} + N_{l,0} - 2N_{l,1}) + \mathrm{Im}(P_R E_R^*)/(2\hbar), \tag{3}$$

$$\frac{\partial N_{l,0}}{\partial \tau} = \sum_k C_{k,0} N_k + \gamma_{\mathrm{PT}}(N_{l,-1} - 2N_{l,0} + N_{l,1}), \tag{4}$$

$$\frac{\partial N_{l,-1}}{\partial \tau} = \sum_k C_{k,-1} N_k + \gamma_{\mathrm{PT}}(-2N_{l,-1} + N_{l,0} + N_{l,1}) + \mathrm{Im}(P_L E_L^*)/(2\hbar), \tag{5}$$

where N_u is the population of the upper level of the lasing transition, $N_{l,m}$ (with $m = 1, 0, -1$) the population of each lower sublevel, and N_k the population of other atomic levels that strongly interact with the lasing ones. The coefficients $C_{j,i}$ denote the collisional (de)excitation and radiative deexcitation rates. The constitutive relation derived from Bloch equations is written as

$$\frac{\partial P_L}{\partial \tau} = \Gamma_L - \gamma P_L - \frac{iE_L}{\hbar} z_{ul}^2 (N_u - N_{l,-1}) + \frac{iE_R}{\hbar} z_{ul}^2 n_i \rho_{1,-1}, \tag{6}$$

$$\frac{\partial P_R}{\partial \tau} = \Gamma_R - \gamma P_R - \frac{iE_L}{\hbar} z_{ul}^2 (N_u - N_{l,1}) + \frac{iE_L}{\hbar} z_{ul}^2 n_i \rho_{1,-1}, \tag{7}$$

$$\frac{\partial n_i \rho_{-1,1}}{\partial \tau} = -\gamma_{-1,1} n_i \rho_{1,-1} + \frac{i}{4\hbar}(P_R^* E_L + P_L E_R^*), \tag{8}$$

where n_i is the density of ions, $\gamma = \pi\Delta\nu$ the full width at half maximum of the transition linewidth, z_{ul} the dipole matrix element, $\rho_{1,-1}$ the off-diagonal matrix element of the states $m = -1, 1$, and $\gamma_{1,-1}$ its relaxation rate. The Stokes parameters, containing all the information about the polarization state of the amplified HH, are directly obtained from the computed fields E_R and E_L with the following formulas:

$$I = |E_R|^2 + |E_L|^2, \qquad Q = 2\mathrm{Re}(E_L^* E_R),$$
$$U = -2\mathrm{Im}(E_R^* E_L), \qquad V = |E_R|^2 - |E_L|^2. \tag{9}$$

Figure 4 shows the calculated evolution of the degree of polarized light and the polarization as the HH pulse propagates and gets amplified in the plasma. Data are taking into account the contribution of the unpolarized ASE collected into the solid angle defined by the amplified HH divergence (FWHM). Polarization states are depicted as the normalized path described in the space by the electric field over an optical period. Figure 4(a) reports that the portion

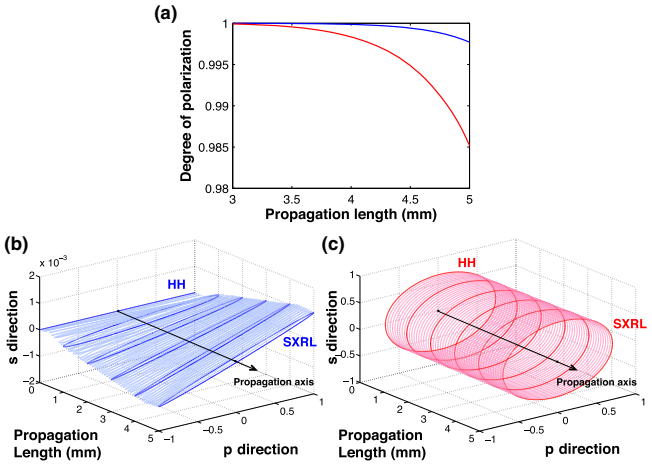

FIG. 4 (color online). (a) Degree of polarized light of amplified HH seeding a plasma-based krypton amplifier. (b) and (c) Evolution of the amplified HH polarization in the case of seeding with linear (blue) and circular (red) polarizations.

of fully polarized light after 5 mm of amplification is over 99.5%. In this fraction, the linearly seeded SXRL polarization [Fig. 4(b)] axis is turned by less than 0.05°, while it gets a very small ellipticity of about 0.04. As far as circularly seeded SXRL is concerned [Fig. 4(c)], the polarization is marginally modified from an initial value of 1 to over 0.98. Those very weak depolarization effects can be explained by off-diagonal elements of the density matrix [Eqs. (6)–(8)], which induce ASE-SXRL coupling resulting in second-order perturbations of the amplified HH polarization. Finally, our numerical modeling is in reasonable agreement with our experimental measurements, substantiating the validity of our approach. Because both HH and SXRL are polarized, the insensitivity of the SXRL signal to the rotation of the analyzer [Figs. 3(c) and 3(d)] provides evidence that the circular polarization state has been maintained over amplification of the 32.8 nm seed HH pulse.

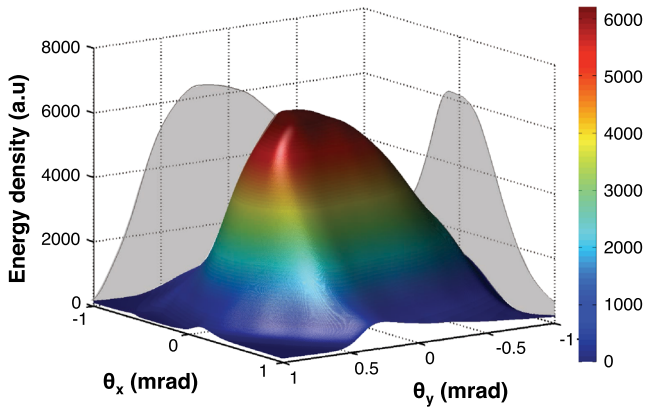

FIG. 5 (color online). Energy distribution of the CPSXRL.

The energy distribution of the 32.8 nm CPSXRL is presented in Fig. 5. The far-field beam profile is nearly Gaussian and has a FWHM divergence of about 1 mrad. The good quality of beam spatial distribution should allow maintaining the advantageous focusing capabilities of the source, as previously measured [20]. The integrated energy distribution of the CPSXRL is found to yield about 10^{10} fully circularly polarized photons, when seeding with about 10^6 circularly polarized photons at 32.8 nm, which corresponds to an amplification factor of nearly 4 orders of magnitude. Despite the low seeding level caused by the poor transmission efficiency of the soft-x-ray polarizer (1.5%), the amplifying properties of the plasma allow efficiently compensating the losses induced by the polarizer transmission.

In conclusion, the demonstrated scheme fills the requirements for a laboratory-scale, jitter-free, and fully circularly polarized photon-rich soft-x-ray coherent source. Being scalable to shorter wavelengths [31] and adaptable to femtosecond SXRL schemes [32,33], the demonstrated approach holds out hope for delivering intense circularly polarized soft-x-ray pulses suitable for photon-demanding measurements in holography [34], crystallography pump-probe experiments [35], and magnetism [36] or circular dichroism in molecular structures [4,8].

We thank J. L. Charles for his technical support. This work was supported by the Agence Nationale de la Recherche, through Projects No. ROLEX ANR-06-BLAN-04 023 01 and No. ANR-10-EQPX-25. We acknowledge funding from project ECOP (Grants No. CZ.1.07/2.3.00/20.0279 and No. CZ.1.07/2.3.00/30.005) and COST Action MP1203.

[1] N. Greenfield, Nat. Protoc. **1**, 2876 (2007).
[2] H. Stoll, A. Puzic, B. Van Waeyenberge, P. Fischer, J. Raabe, M. Buess, T. Haug, R. Hollinger, C. Back, D. Weiss, and G. Benbeaux, Appl. Phys. Lett. **84**, 3328 (2004).
[3] G. Contini, S. Turchini, S. Sanna, D. Catone, J. Fujii, I. Vobornik, T. Prosperi, and N. Zema, Phys. Rev. B **86**, 035426 (2012).
[4] G. Garica, L. Nahon, S. Daly, and I. Powis, Nat. Commun. **4**, 2132 (2010).
[5] X. Zhou, R. Lock, N. Wagner, W. Li, H. C. Kapteyn, and M. M. Murnane, Phys. Rev. Lett. **102**, 073902 (2009).
[6] A. Fleischer, O. Kfir, T. Diskin, P. Sidorenko, and O. Cohen, Nat. Photonics **8**, 543 (2014).
[7] G. Lambert, B. Vodungbo, J. Gautier, B. Mahieu, V. Malka, S. Sebban, P. Zeitoun, J. Luning, J. Perron, A. Andreev, S. Stremoukhov, F. Ardana-Lamas, A. Dax, C. Hauri, A. Sardinha, and M. Fajardo, Nat. Commun. **6**, 6167 (2015).
[8] A. Ferré, C. Handschin, D. Dumergue, F. Burgy, A. Comby, D. Deschamps, B. Fabre, G. Garcia, R. Gréneaux, L. Merceron, E. Mével, L. Nahon, S. Petit, B. Pons, D. Staedter, S. Weber, T. Ruchon, V. Blanchet, and Y. Mairesse, Nat. Photonics **9**, 93 (2014).

[9] J. Bahrt, A. Gaupp, W. Gudat, M. Mast, K. Molter, W. Peatman, M. Scheer, T. Schroter, and C. Wang, Rev. Sci. Instrum. **63**, 339 (1992).
[10] E. A. Schneidmiller and M. V. Yurkov, Phys. Rev. ST Accel. Beams **16**, 110702 (2013).
[11] H. Deng, T. Zhang, L. Feng, C. Feng, B. Liu, X. Wang, T. Lan, G. Wang, W. Zhang, X. Liu, J. Chen, M. Zhang, G. Lin, M. Zhang, D. Wang, and Z. Zhao, Phys. Rev. ST Accel. Beams **17**, 020704 (2014).
[12] E. Allaria, B. Diviacco, C. Callegari, P. Finetti, B. Mahieu, J. Viefhaus, M. Zangrando, G. De Ninno, G. Lambert, E. Ferrari, J. Buck, M. Ilchen, B. Vodungbo, N. Mahne, C. Svetina, C. Spezzani, S. Di Mitri, G. Penco, M. Trovó, W. M. Fawley *et al.*, Phys. Rev. X **4**, 041040 (2014).
[13] B. Rus, T. Mocek, A. R. Prag, M. Kozlova, G. Jamelot, A. Carillon, D. Ros, D. Joyeux, and D. Phalippou, Phys. Rev. A **66**, 063806 (2002).
[14] N. Hasegawa, A. Sasaki, H. Yamatani, M. Kishimoto, M. Tanaka, Y. Ochi, M. Nishikino, Y. Kuneida, and T. Kawachi, J. Opt. Soc. Korea **13**, 60 (2009).
[15] T. Kawachi, K. Murai, G. Yuan, S. Ninomiya, R. Kodama, H. Daido, Y. Kato, and T. Fujimoto, Phys. Rev. Lett. **75**, 3826 (1995).
[16] P. Zeitoun, G. Faivre, S. Sebban, T. Mocek, A. Hallou, M. Fajardo, A. Aubert, P. Balcou, F. Burgy, D. Douillet, S. Kazamias, G. de Lachèze-Murel, T. Lefrou, S. le Pape, P. Mercière, H. Merdji, A. Morlens, J. Rousseau, and C. Valentin, Nature (London) **431**, 426 (2004).
[17] Y. Wang, E. Granados, M. A. Larotonda, M. Berrill, B. M. Luther, D. Patel, C. S. Menoni, and J. J. Rocca, Phys. Rev. Lett. **97**, 123901 (2006).
[18] S. Sebban, T. Mocek, D. Ros, L. Upcraft, P. Balcou, R. Haroutunian, G. Grillon, B. Rus, A. Klisnick, A. Carillon, G. Jamelot, C. Valentin, A. Rousse, J. P. Rousseau, L. Notebaert, M. Pittman, and D. Hulin, Phys. Rev. Lett. **89**, 253901 (2002).
[19] D. G. Lee, J.-H. Kim, K.-H. Hong, and C. H. Nam, Phys. Rev. Lett. **87**, 243902 (2001).
[20] J. Goddet, S. Sebban, J. Gautier, P. Zeitoun, C. Valentin, F. Tissandier, T. Marchenko, G. Lambert, M. Ribieres, D. Douillet, T. Lefrou, G. Iaquaniello, F. Burgy, G. Maynard, B. Cros, B. Robillard, T. Mocek, J. Nejdl, M. Kozlova, and K. Jakubczak, Opt. Lett. **34**, 2438 (2009).
[21] T. Mocek, S. Sebban, G. Maynard, P. Zeitoun, G. Faivre, A. Hallou, M. Fajardo, S. Kazamias, B. Cros, D. Aubert, G. de Lacheze-Murel, J. P. Rousseau, and J. Dubau, Phys. Rev. Lett. **95**, 173902 (2005).
[22] P. Hochst, R. Patel, and F. Middleton, Nucl. Instrum. Methods Phys. Res., Sect. A **347**, 107 (1994).
[23] B. Vodungbo, A. Barszczak Sardinha, J. Gautier, G. Lambert, C. Valentin, M. Lozano, G. Iaquaniello, F. Delmotte, S. Sebban, J. Luning, and P. Zeitoun, Opt. Express **19**, 4346 (2011).
[24] E. Oliva, P. Zeitoun, M. Fajardo, G. Lambert, D. Ros, S. Sebban, and P. Velarde, Phys. Rev. A **84**, 013811 (2011).
[25] Y. Wang, S. Wang, E. Oliva, L. Li, M. Berrill, L. Yin, Y. Nejdl, B. Luther, C. Proux, T. Le, J. Dunn, D. Ros, P. Zeitoun, and J. Rocca, Nat. Photonics **8**, 381 (2014).
[26] O. Larroche, D. Ros, A. Klisnick, A. Sureau, C. Moller, and H. Guennou, Phys. Rev. A **62**, 043815 (2000).
[27] B. Cros, T. Mocek, I. Bettaibi, G. Vieux, M. Farinet, J. Dubau, S. Sebban, and G. Maynard, Phys. Rev. A **73**, 033801 (2006).
[28] A. Sureau and P. B. Holden, Phys. Rev. A **52**, 3110 (1995).
[29] C. M. Kim, J. Lee, and K. A. Janulewicz, Phys. Rev. Lett. **104**, 053901 (2010).
[30] C. M. Kim, K. A. Janulewicz, and J. Lee, Phys. Rev. A **84**, 013834 (2011).
[31] M. Berrill, D. Alessi, Y. Wang, S. Domingue, D. Martz, B. Luther, Y. Liu, and J. Rocca, Opt. Lett. **35**, 2317 (2010).
[32] D. V. Korobkin, C. H. Nam, S. Suckewer, and A. Goltsov, Phys. Rev. Lett. **77**, 5206 (1996).
[33] S. J. Moon and D. C. Eder, Phys. Rev. A **57**, 1391 (1998).
[34] S. Eisebitt, J. Luning, F. Schlotter, M. Lorgen, O. Hellwig, W. Eberhardt, and J. Stohr, Nature (London) **432**, 885 (2004).
[35] S. Boutet, L. Lomb, G. Williams, T. Barends, A. Aquilla, R. Doak, U. Weierstall, D. DePonte, J. Steinbrener, R. Schoeman, M. Messerschmitt, A. Barty, T. White, S. Kassemayer, R. Kirian, M. Steibert, P. Montanez, C. Kenney, R. Herbst, P. Hart *et al.*, Chirality **337** (2012).
[36] B. Vodungbo, J. Gautier, G. Lambert, A. Barszczak Sardinha, M. Lozano, S. Sebban, M. Ducousso, W. Boutu, K. Li, B. Tudu, M. Tortarolo, R. Hawaldar, R. Delaunay, V. Lopez-Flores, J. Arabski, C. Boeglin, H. Merdji, P. Zeitoun, and J. Luning, Nat. Commun. **3**, 999 (2012).